DOI:10.1158/0008-5472.CAN-06-1728

Cancer Research

Magnetic Resonance Visualization of Tumor Angiogenesis by Targeting Neural Cell Adhesion Molecules with the Highly Sensitive Gadolinium-Loaded Apoferritin Probe

Simonetta Geninatti Crich, Benedetta Bussolati, Lorenzo Tei, et al.

Cancer Res 2006;66:9196-9201. Published online September 18, 2006.

DOI:10.1158/0008-5472.CAN-06-1728

Research Article

Magnetic Resonance Visualization of Tumor Angiogenesis by Targeting Neural Cell Adhesion Molecules with the Highly Sensitive Gadolinium-Loaded Apoferritin Probe

Simonetta Geninatti Crich,[1] Benedetta Bussolati,[2] Lorenzo Tei,[1] Cristina Grange,[2] Giovanna Esposito,[1] Stefania Lanzardo,[3] Giovanni Camussi,[2] and Silvio Aime[1]

[1]Department of Chemistry IFM and Center for Molecular Imaging, University of Torino; [2]Department of Internal Medicine and Research Center for Experimental Medicine, University of Torino, Torino, Italy; and [3]Department of Clinical and Biological Sciences, University of Torino, Orbassano, Italy

Abstract

Tumor vessel imaging could be useful in identifying angiogenic blood vessels as well as being a potential predictive marker of antiangiogenic treatment response. We recently reported the expression of the neural cell adhesion molecule (NCAM) in the immature and tumor endothelial cell (TEC) lining vessels of human carcinomas. Exploiting an *in vivo* model of human tumor angiogenesis obtained by implantation of TEC in Matrigel in severe combined immunodeficiency mice, we aimed to image angiogenesis by detecting the expression of NCAM with magnetic resonance imaging. The imaging procedure consisted of (*a*) targeting NCAMs with a biotinylated derivative of C3d peptide that is known to have high affinity for these epitopes and (*b*) delivery of a streptavidin/gadolinium (Gd)-loaded apoferritin 1:1 adduct at the biotinylated target sites. The remarkable relaxation enhancement ability of the Gd-loaded apoferritin system allowed the visualization of TEC both *in vitro* and *in vivo* when organized in microvessels connected to the mouse vasculature. Gd-loaded apoferritin displayed good *in vivo* stability and tolerability. The procedure reported herein may be easily extended to the magnetic resonance visualization of other epitopes suitably targeted by proper biotinylated vectors. (Cancer Res 2006; 66(18): 9196-201)

Introduction

Among the available "*in vivo*" diagnostic modalities, magnetic resonance imaging (MRI) is the most powerful technique thanks to its superb anatomic resolution (<100 μm) and its ability to report on both the structure and function of soft tissues (1). Moreover, the use of contrast agents could further enhance the differences between healthy and diseased tissues (2, 3). Gadolinium (Gd)-based contrast agents are the most used systems in both clinical and experimental settings, however, the commercially available Gd contrast agents are only extracellular agents endowed with a nonspecific biodistribution. The development of new Gd-based contrast agents with high contrast ability and targeting capability is the key step for the set-up of innovative magnetic resonance-molecular imaging (MRMI) protocols (4–7).

In fact, in MRMI procedures, one has to visualize epitopes that are present at very low concentrations (typically in the 50-100 nmol/L range), and therefore, it is necessary to design proper methods to amplify the response upon recognition of the target of interest. In this work, we have applied a targeting procedure aimed at visualizing tumor endothelial cells (TEC) by using the recently described Gd-loaded apoferritin system as an imaging reporter (8). Each Gd-HPDO3A entrapped in the apoferritin cavity displays the highest relaxivity peak reported thus far (~ 80 mmol/L^{-1} s^{-1}), and the amplification effect is further enhanced by the presence of 8 to 10 molecules of Gd-HPDO3A per apoferritin unit (8). In order to develop a system of general applicability, the outer surface of the Gd-loaded apoferritin was biotinylated so that it could be delivered to the site of interest by means of a well-established avidin/biotin recognition pathway. Many efforts have already been devoted to develop a MRMI protocol for the visualization of neoformed vessels in the tumor region (9, 10). Angiogenesis has a crucial role in tumor growth, metastasis, and inflammatory diseases; therefore, targeting epitopes hyperexpressed in the neovasculature is of great interest for the early detection of tumors and the follow-up of therapeutic treatments (11, 12). The most investigated systems have dealt with the visualization of integrin receptors (13–18), E-selectin (19, 20), and intercellular cell adhesion molecule-1 (21).

We have recently described the isolation and characterization of renal tumor–derived endothelial cells (22). *In vivo* in severe combined immunodeficiency (SCID) mice, TEC organize within Matrigel in a network of small vessels connected with the mouse vasculature, providing an *in vivo* model of human tumor angiogenesis. TEC, but not normal endothelial cells, expressed both *in vitro* and *in vivo*, the neural cell adhesion molecule (NCAM), an adhesion molecule of the immunoglobulin superfamily (23) largely expressed by embryonic tissue. NCAM is transiently re-expressed during angiogenic endothelial cell differentiation and organization, and is stably expressed by TECs (24).

As a targeting vector for TEC, we used a specific NCAM-binding peptide, C3d (25–28). Therefore, using this peptide coupled to the Gd-loaded apoferritin by the biotin/streptavidin system, we have constructed a molecular imaging probe that we have tested on TEC *in vitro* and on TEC-formed vessels *in vivo* in SCID mice.

Materials and Methods

Gd-HPDO3A (Prohance) was kindly provided by Bracco S.p.A. Apoferritin (Milan, Italy) and all other chemicals were purchased from Sigma-Aldrich (St. Louis, MO). The longitudinal water proton relaxation rate was measured on a Stelar Spinmaster spectrometer (Stelar, Mede, Italy).

Gd-loaded apoferritin preparation. The loading of paramagnetic chelates in the apoferritin cavity was carried out as described previously (8). Briefly, the dissociation of the apoferritin into its subunits was done by

Requests for reprints: Silvio Aime, Department of Chemistry IFM, University of Torino, via P. Giuria 7, Turin 10125, Italy. Phone: 39-11670-7520; Fax: 39-11670-7855; E-mail: silvio.aime@unito.it.

doi:10.1158/0008-5472.CAN-06-1728

DOI:10.1158/0008-5472.CAN-06-1728

lowering the pH of the protein solution (to pH 2; 1×10^{-5} mol/L) using 1 mol/L of HCl and maintaining this low pH for about 15 minutes. Afterwards, the Gd-HPDO3A complex was added to the solution at a 0.1 mol/L concentration, and successively, the pH was adjusted to 7.4 using 1 mol/L of NaOH. The resulting solution was stirred at room temperature for ~2 hours and then dialyzed against HEPES buffer saline [HEPES 5 mmol/L, NaCl 0.1 mol/L (pH 7.4)] to remove Gd-HPDO3A molecules not trapped inside the protein shell. At the end, the solution was filtered with a 0.2 μm membrane filter.

Biotinylation of the Gd-loaded apoferritin. The biotinylation of Gd-loaded apoferritin was carried out using NHS-LC-BIOTIN [*N*-(+)-biotinyl-6-aminocaproic acid *N*-succinimidyl ester] according to standard protein modification protocols (29). Briefly, 1.6 μmol of NHS-LC-BIOTIN previously dissolved in DMF were added to a Gd-loaded 8 μmol/L apoferritin solution (10 mL). Afterwards, the solution was stirred for 30 minutes at room temperature and then dialyzed against HEPES buffer saline to remove the unbound NHS-LC-BIOTIN reagent. After dialysis, the ratio of biotin/apoferritin was of 5 ± 1 biotin residues per apoferritin molecule as determined with the HABA colorimetric assay (29). Finally, the biotinylated Gd-loaded apoferritin (Gd-Apo-Bio) solution was concentrated to ~80 to 120 μmol/L using Vivaspin 500 centrifugal filters with a membrane pore size of M_r 50,000.

The final protein concentration of each sample was determined by the Bradford method (30) using bovine serum albumin as the standard. The residual Gd-HPDO3A concentrations ranging from 0.8 to 1.2 mmol/L were determined by inductively coupled plasma-mass spectrometry (ICP-MS, Element-2; Thermo-Finnigan, Rodano, Milan, Italy). A single ICP-MS measurement represents the average of three replicates from the same sample (previously digested in concentrated nitric acid).

Synthesis of C3d-Bio NCAM mimetic peptide. The synthesis of the biotinylated peptide ligand of the NCAM Ig1 module (C3d-Bio) was accomplished as described previously (24). Briefly, C3d-Bio (Scheme) was synthesized using the standard Fmoc strategy with a Fmoc-Lys (Fmoc)-OH (EMD Biosciences, San Diego, CA) core and a Fmoc-PAL-PEG-PS (Applied Biosystems, Foster City, CA) resin. The biotinylation step was carried out in solid phase using D-Biotin and HATU/DIPEA. A good yield (60%) of the final Cd3-Bio peptide was obtained after cleavage from the resin, precipitation with diethyl ether, and subsequent purification with semipreparative high-performance liquid chromatography (Atlantis RPC18, 19/100, purity >90%; Waters, Milford, MA). HABA colorimetric assay confirmed that four biotin residues were attached to the C3d dendrimeric peptide (29).

Tumor-derived endothelial cells. TEC were isolated from specimens of clear cell–type renal cell carcinomas using anti-CD105 antibodies coupled to magnetic beads, by magnetic cell sorting using the MACS system (Miltenyi Biotec), as previously described (22). TEC cell lines were established renal carcinomas and maintained in culture in EBM complete medium supplemented with epidermal growth factor (10 ng/mL), hydrocortisone (1 mg/mL), bovine brain extract (all from Cambrex Bioscience, East Rutherford, NJ), and 10% FCS. TEC were previously characterized as endothelial cells by morphology, positive staining for vWF antigen, CD105, CD146, vascular endothelial-cadherin, and negative staining for cytokeratin and desmin.

Binding experiments. For the *in vitro* binding experiments, TEC were harvested using a nonenzymatic dissociation solution (Sigma), washed with PBS, counted in a microcytometer chamber, and resuspended in DMEM (2×10^6 in 250 μL of DMEM). C3d-Bio peptide, streptavidin, and Gd-loaded/apoferritin were sequentially added to TEC at a molar ratio of 20:1:1 (at 20°C), with a 20-minute time interval between the addition of each component. After each binding step, the cells were washed thrice with 5 mL of ice-cold PBS. The amount of Gd bound to cells was measured by ICP-MS. The extent of aspecific binding of streptavidin/biotinylated Gd-loaded apoferritin was assessed by repeating the above experiments without the addition of the targeting peptide. MR images were acquired at 7 T on glass capillaries containing cell pellets placed in an agar phantom.

***In vivo* model of human tumor angiogenesis.** For the *in vivo* studies, TEC were implanted s.c. into SCID mice (Charles River) within growth factor–reduced Matrigel, as previously described (22). Cells were harvested using nonenzymatic dissociation solution (Sigma), washed with PBS, and resuspended in DMEM (1×10^6 in 250 μL DMEM). Cells were chilled on ice, added to 250 μL of Matrigel at 4°C and injected s.c. into the left posterior side of SCID mice via a 26-gauge needle using a 1 mL syringe. On day 6, previously reported as the requested time for connection between mice and human microvessels, mice were processed for MRI experiments.

MRI. MR images were acquired on a Bruker Avance 300 spectrometer (7 T) equipped with a Micro 2.5 microimaging probe. The image of cell pellets was obtained using a standard T_1-weighted multislice multiecho sequence (TR/TE/NEX = 200/3.3/8; FOV, 1.2 cm; one slice, 1 mm; in-plane resolution, 94 × 94 μm).

Mice (n = 6) were treated i.v. with C3d-Bio or with the vehicle alone (n = 4), followed by the administration of biotinylated Gd-loaded apoferritin (Gd-Apo-Bio) and streptavidin. In selected experiments, streptavidin was replaced with FITC-labeled streptavidin (Sigma). The amount of the C3d-Bio (20 μmol/kg) administered to the first group of mice was 20 times higher than the amount of streptavidin (1 μmol/kg) and Gd-Apo-Bio (1 μmol/kg) in order to pursue the highest binding to the target molecules on tumor cells. To allow the removal of the unbound peptide from the circulation, the administration of streptavidin and Gd-Apo-Bio was done ~45 minutes after the C3d-Bio injection. Gd-loaded apoferritin and streptavidin were administered together on the assumption that, being present in a 1:1 molar ratio, each streptavidin molecule still has three binding sites available for anchoring to the biotin residues on C3d-Bio pretargeted to the tumor cells. Fat-suppressed T_1-weighted spin echo MR images (TR/TE/NEX = 250/3.2/6; FOV, 2.8 cm; one slice, 1 mm; in-plane resolution, 220 × 220 μm) were recorded before, 10 minutes, 5, 24, and 48 hours after contrast administration. Fat suppression was done by applying a presaturation pulse (90 degrees BW = 1,400 Hz) at the absorption frequency of fat (−1,100 Hz from water). The mean signal intensity (SI) enhancement was evaluated on the regions of interest which were manually drawn around the tumor. The SI measured on each image was normalized using a standard Gd solution. Hyperintense regions were defined including all pixels with a SI increased by >3 SD of the precontrast tumor. For statistical analysis, one-way Student's t test was used. Probability values <0.05 were considered statistically different.

Histology of dissected plugs. Five hours after treatment, mice were sacrificed, and tumor endothelial plugs were recovered and processed for histology and immunofluorescence. Typically, the overlying skin was

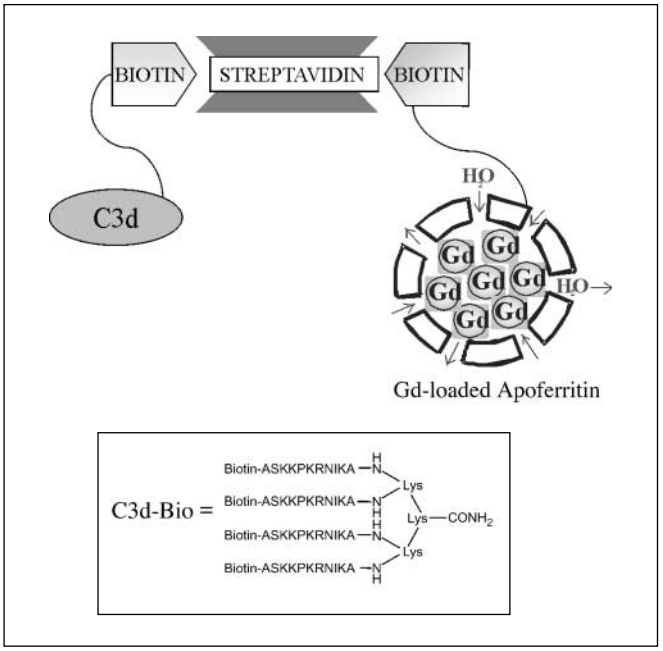

Scheme. Schematic representation of the adduct formed by C3d-Bio, streptavidin, and biotinylated Gd-loaded apoferritin (Gd-Apo-Bio). The sequence of the dendrimeric C3d-Bio NCAM mimetic peptide is outlined.

DOI:10.1158/0008-5472.CAN-06-1728

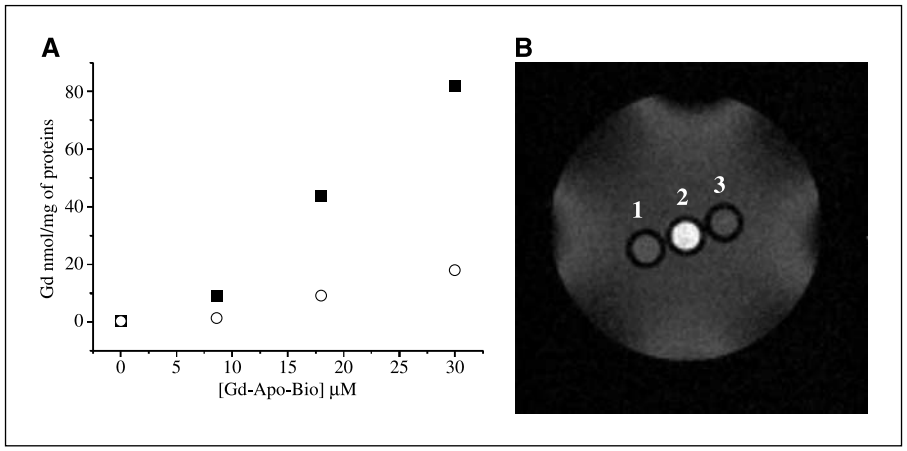

Figure 1. *A,* binding of biotinylated Gd-loaded apoferritin to TEC in the presence (■) and in the absence (○) of C3d-Bio. The amount of Gd bound to TEC determined by ICP-MS is significantly higher when cells were incubated with C3d-Bio. *B,* T_1-weighted spin echo MR image (measured at 7 T), of an agar phantom containing: TEC incubated (20 minutes at 20°C) with streptavidin and Gd-Apo-Bio (30 μmol/L) in the absence (*1*) and in the presence (*2*) of C3d-Bio (600 μmol/L) and unlabeled TEC (*3*). The relaxation rate measured for TEC incubated with C3d-Bio, streptavidin, and biotinylated Gd-loaded apoferritin was 1.3 s^{-1}, corresponding to a SI enhancement of 200% with respect to the unlabeled cells. The R_{1obs} of the cells incubated only with streptavidin and Gd-Apo-Bio was 0.505 s^{-1}, only 10% higher than the relaxation rate measured for the untreated control cells (0.46 s^{-1}).

removed, and gels were cut out by retaining the peritoneal lining for support, fixed in 10% buffered formalin and embedded in paraffin. Sections (3 μm) were cut, stained with H&E, and examined under a light microscope system to detect the vascular network formed by TEC. In parallel, sections were observed under immunofluorescence microscope to detect FITC-conjugated streptavidin linked to C3d-bio. FITC was amplified by the use of an anti-FITC polyclonal antibody (Molecular Probes, Leiden, the Netherlands), followed by FITC-labeled anti-rabbit goat antibodies (Sigma). The nature of the vessels formed by TEC was evidenced by positive immunofluorescence staining for human HLA class I antigen using anti-HLA antibodies (BioLegend, San Diego, CA).

Results

Preparation and characterization of the biotinylated Gd-loaded apoferritin. Apoferritin (Scheme), loaded with about 8 to 10 molecules of the commercially available Gd-HPDO3A, was prepared according to the method previously reported (8). The paramagnetic complex, inside the protein cavity, shows an outstanding high millimolar relaxivity of $\sim 70 \pm 10$ mmol/L^{-1} s^{-1} at 20 MHz and 25°C, which is ~20 times higher than that observed in pure water. It has been recently shown that a large contribution to the outstanding relaxivity of this system arises from the interaction of the paramagnetic complex with the exchangeable protons (and likely the hydration water) on the protein surface of the inner cavity of apoferritin (31). For the purpose of developing a targeting procedure based on the well known biotin/avidin recognition pathway, Gd-loaded apoferritin was biotinylated using the commercially available NHS-LC-BIOTIN reagent. The protein possesses several $-NH_2$ groups available for conjugation with the NHS-LC-BIOTIN. After dialysis, the ratio of biotin/apoferritin was 5 ± 1 biotin residues per apoferritin molecule as determined by the HABA colorimetric assay (29). The relaxivity of Gd-HPDO3A inside the cavity did not change after the conjugation reaction.

"*In vitro*" MR imaging of tumor-derived endothelial cells. It is well established that NCAM molecules are the targets for the C3d peptide (25–28). The latter peptide is easily biotinylated in solid phase at the four-terminal NH_2 by the standard Biotin/HATU/DIPEA method to obtain C3d-Bio in good yield.

We previously showed the specificity and the dose-dependent binding of the C3d-Bio peptide to TEC (and not to normal endothelial cells) by cytofluorimetric analysis (24). Here, we investigate the MRI visualization of the C3d-Bio binding to TEC using streptavidin and biotinylated Gd-loaded apoferritin. As shown in Fig. 1*A*, the amount of Gd bound to cell membranes in the presence of C3d-Bio is significantly higher than that found in the aspecific binding experiments, at any concentration of Gd-loaded apoferritin added to the incubation medium. T_1-weighted spin-echo image (Fig. 1*B*) showed that TEC incubated with the three components (C3d-Bio, streptavidin, and biotinylated Gd-loaded apoferritin) seem to be hyperintense with respect to the control cells. The maintenance of the Gd-Apo-Bio integrity upon binding to the cell membrane has been assessed by measuring the $1/T_1$ nuclear magnetic resonance dispersion (NMRD) profile over a range of Larmor frequencies. In fact, Gd-loaded apoferritin has a profile characterized by a relaxivity hump at ~35 MHz, typical of slowly moving systems, whereas the relaxivity of free Gd-HPDO3A, at frequencies >5 MHz, is constant at any value of the applied field. On the basis of the $1/T_1$ data acquired from 0.23 to 2.0 T, one can see that the relaxivity of the Gd-loaded apoferritin bound to TEC displays the same bell-shaped behavior detected in water (Fig. 2). On the contrary, at the expected value of ~5 mmol/L^{-1} s^{-1}, the relaxivity of Gd-HPDO3A added to the untreated cellular pellet is constant over all the magnetic field ranges tested. Because the relaxivity peak shown in Fig. 2 occurs only when the Gd-HPDO3A complex is internalized

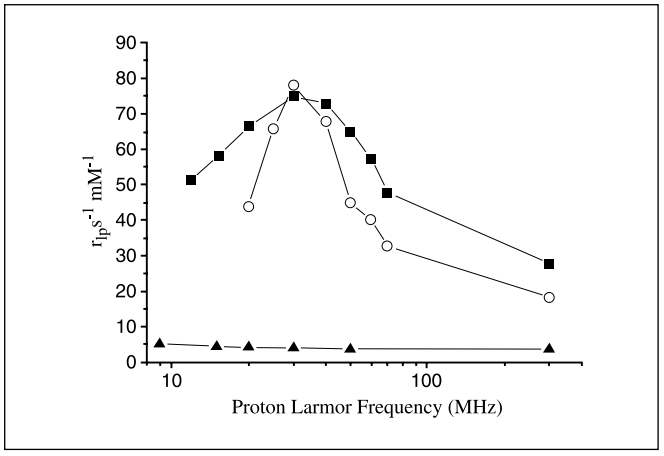

Figure 2. $1/T_1$ ^{1}H-NMRD profile [9-300 MHz (pH 7) and 25°C] of free Gd-HPDO3A (▲) compared with Gd-loaded apoferritin before (■) and after binding to TEC (○). Gd-loaded apoferritin has a profile characterized by a relaxivity peak typical of slowly moving systems, whereas the relaxivity of free Gd-HPDO3A is constant at any value of the applied field. The Gd-Apo-Bio relaxivity peak was also observed after binding to the cell membrane, thus demonstrating the maintenance of the protein shell.

DOI:10.1158/0008-5472.CAN-06-1728

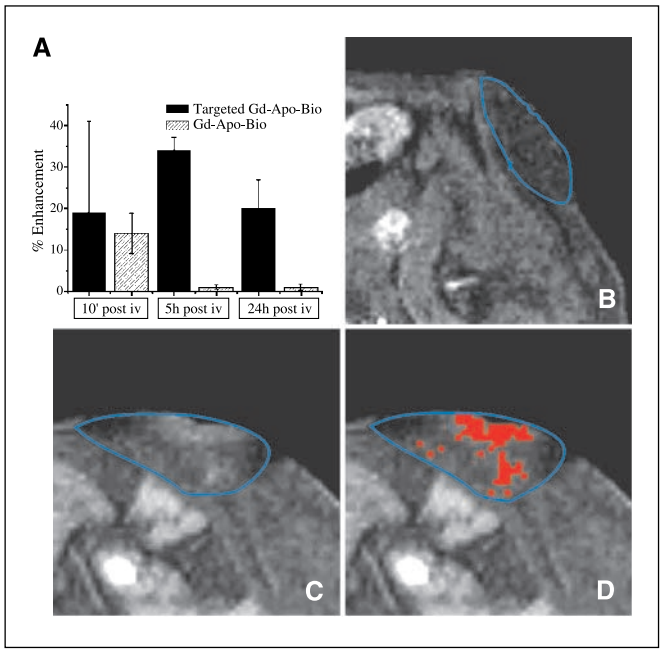

Figure 3. *A,* MRI SI enhancement of tumors in SCID mice grafted with TEC treated with Gd-loaded apoferritin targeted and nontargeted to NCAM. MR T_1-weighted images of tumors done before (*B*) and 5 hours after (*C* and *D*) the administration of C3d-Bio/streptavidin/Gd-loaded apoferritin (20:1:1), which corresponds to a Gd dose of 0.01 mmol/kg. The tumors are outlined in blue, red highlights the areas where the signal is 3 SD more intense than the precontrast tumor intensity (*D*). Marked SI enhancement (>30%) was measured in the region of interest corresponding to the whole tumor 5 hours after the injection of Gd-Apo-Bio pretargeted with the C3d-Bio peptide.

in the apoferritin cavity, we can conclude that the Gd-loaded apoferritin remains intact after binding to the cell membrane.

"*In vivo*" MRI of TEC-formed vessels. In order to assess the *in vivo* capability of the Gd-loaded apoferritin to visualize human tumor vessels by selectively targeting a TEC surface marker, a MRI study was carried out on SCID mice grafted with TEC. After 6 days, TEC organized in capillary structures, as previously described (22). All the experiments were done at this time point (6 days after implantation), when human tumor vessels were shown to be connected with the murine vasculature. Mice were treated i.v. with C3d-Bio (or with the vehicle alone) followed, after 45 minutes, by the administration of streptavidin and Gd-Apo-Bio. Fat-suppressed T_1-weighted multislice multiecho MR images were recorded before, 10 minutes, 5, 24, and 48 hours after the contrast administration. In Fig. 3*A*, the tumor SI measured on two different groups of mice were compared 5 and 24 hours after the administration of the imaging probe. Marked SI enhancement (>30%) was measured in the region of interest corresponding to the whole tumor 5 hours after the injection of Gd-Apo-Bio pretargeted with the C3d-Bio peptide. On the contrary, no significant difference with the pretreatment image (3-5%) was measured after the injection of Gd-Apo-Bio alone, indicating that the nonspecific probe accumulation was below the detection limit. After 24 hours, the SI enhancement decreases to 20%, but the difference between the two groups of animals remains significant (P = 0.0034). Figure 3 shows the T_1-weighted MR image of the tumor region obtained 5 hours after the administration of the streptavidin/Gd-Apo-Bio constructs in the presence and in the absence of the pretargeting with C3d-Bio. In Fig. 3*C*, the red-colored pixels are those showing a SI increased by >3 SD of the precontrast tumor. These enhanced pixels represent ~24% of the total tumor pixels in the first group of mice, whereas in the second group, they represent only 1%.

The SI enhancements measured on the liver, kidneys, and muscle upon administration of the streptavidin/Gd-Apo-Bio construct show that the elimination of the Gd-loaded apoferritin occurs largely through the liver (Fig. 4). The i.v. injection of the same dose of Gd-HPDO3A showed that the liver SI remains unchanged (data not shown) as expected for this neutral and highly hydrophilic contrast agent whose excretion occurs only through the kidneys (32). This observation is further evidence of the maintenance of a Gd complex inside the apoferritin cavity, which then follows the protein elimination pathways through liver uptake.

The *in vivo* binding of C3d-Bio NCAM mimetic peptide at the TEC neoformed vessels was confirmed by immunofluorescence following *in vivo* administration of FITC-labeled streptavidin/Gd-Apo-Bio. As shown in Fig. 5, the C3d-Bio peptide was detected by the FITC-labeled streptavidin/Gd-Apo-Bio complex as fluorescent dots underlining the human neoformed vessels. The normal murine renal endothelium (Fig. 5*C*), as well as the endothelium of skeletal muscles (data not shown) used as controls, were negative.

Discussion

An important application in molecular imaging is the detection of neoangiogenesis in tumors. For this purpose, the development of highly efficient MRI contrast agents has to be combined with the use of specific vectors able to carry the imaging reporter to the target site. In this work, NCAM was chosen as a selective marker of TECs as it is not expressed by normal quiescent endothelial cells

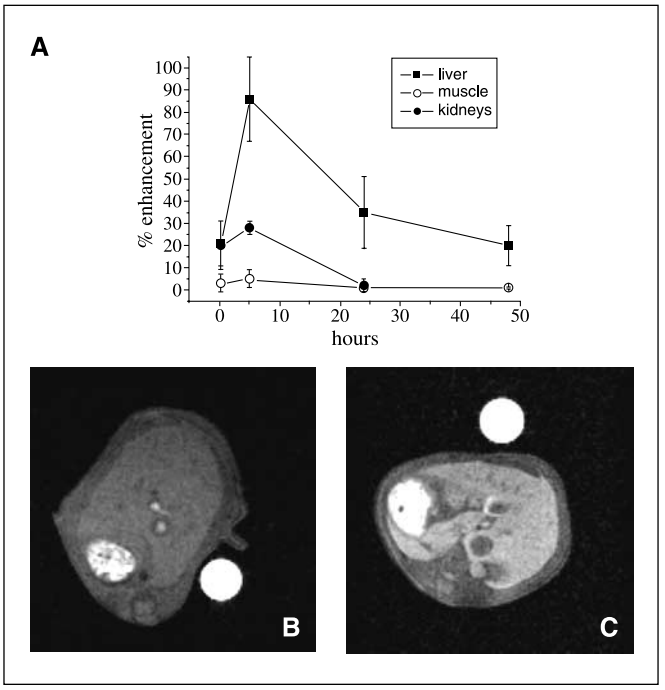

Figure 4. *A,* time course of MRI SI enhancement of liver (■), kidneys (●), and muscle (○) measured on tumor-bearing mice after Gd-loaded apoferritin administration. T1-weighted MR images of mouse liver acquired before (*B*) and after (*C*) 5 hours after the administration of Gd-loaded apoferritin. The data represent the cumulative values from the two groups of mice, i.e., treated and untreated with C3d-Bio. These images show that the elimination of the imaging probe occurs largely through the liver.

DOI:10.1158/0008-5472.CAN-06-1728

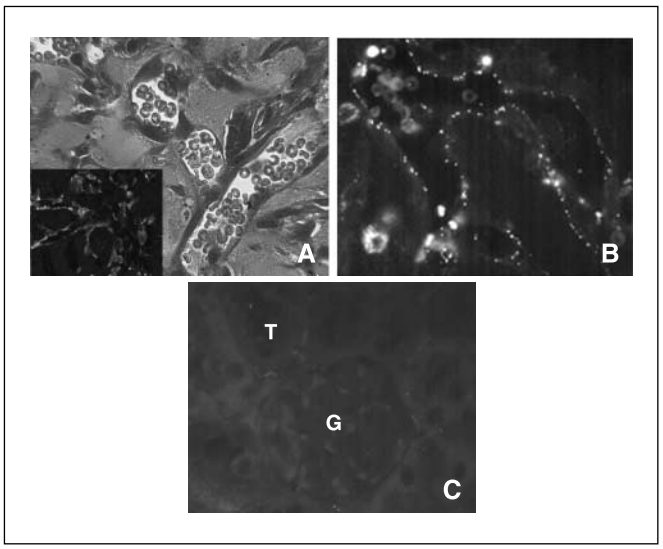

Figure 5. Immunofluorescence detection of *in vivo* localization of C3d-Bio peptide in human vessels formed by TEC in SCID mice. The same Matrigel plugs in which localization of C3d-Bio was observed by MRI was submitted to histologic and immunofluorescence examination. *A,* light microscopy micrographs representative of vessels formed by TEC within Matrigel. The neoformed vessels show a patent lumen containing erythrocytes, indicating the connection to the murine vasculature. The nature of the vessels is indicated by the expression of human class I antigens (*inset*). *B,* immunofluorescence detection of NCAM binding by *in vivo* injection of C3d-Bio followed by the complex FITC-streptavidin/Gd-Apo-Bio, as described in Materials and Methods. Granular fluorescence is detectable along the surface of vessels. *C,* absence of NCAM binding in the glomerular and peritubular capillaries of the mouse kidney, used as control. Three experiments were done with similar results.

(Fig. 5). The synthetic peptide ligand of the NCAM Ig1 module, identified few years ago by Rønn et al. (25), was used as a specific vector for the imaging probe. TECs express several receptors and adhesion molecules that are absent or barely detectable in normal vessels (12), providing the basis for antiangiogenic therapy. Among those, NCAM expression by human tumor–associated endothelial cells is of particular interest, as it identifies immature endothelial cells in tumors and not normal endothelial cells (22). In addition, we showed that targeting NCAM with a saporin-conjugated NCAM peptide induced a cytotoxic effect on TEC but not on normal endothelial cells (24). These data suggested that NCAM could be exploited as a new marker expressed by endothelial cells with an angiogenic phenotype and that targeting of NCAM could be useful both as antiangiogenic therapy and as molecular imaging probe.

With regard to the imaging probe, the system formed by the entrapment of Gd-HPDO3A into the cavity of apoferritin seems to have several favorable properties, i.e., (*a*) one of the highest relaxivity peaks reported thus far (8); (*b*) low toxicity, because the highly stable Gd-HPDO3A is a neutral, highly hydrophilic, well-tolerated contrast agent (33, 34), and apoferritin, being an endogenous protein, does not cause any immune response; and (*c*) high stability of the protein quaternary structure (35), which allows an easy functionalization of the exposed amino groups in order to endow the system with specific recognition capabilities.

The outstanding high relaxivity of the Gd-HPDO3A is the result of the amplification of dipolar interactions occurring at the large surface area of the inner cavity of the protein (with a diameter of 7-8 nm) in which Gd-HPDO3A is entrapped (~8-10 per apoferritin), whereas the water molecules are freely exchanging with the "bulk" solvent. Thus, this highly efficient system, containing a Gd(III) complex with a relaxivity ~20 times higher than that shown by commercially available contrast agents, seems to be a particularly suitable candidate for molecular imaging at the cellular level. The efficiency of the Gd-loaded apoferritin to deliver Gd units to the target has been tested on hepatocytes which bind ferritin with high affinity through two receptor classes (5).

Although one may envisage a number of ways to deliver the Gd-loaded apoferritin to the target receptor sites, in this article, we considered a well known and versatile procedure based on the biotin/streptavidin recognition path. In fact, using the streptavidin unit as a linker between the biotinylated Gd-loaded apoferritin (Gd-Apo-Bio) and the biotinylated targeting peptide, it is possible to address the imaging reporters at the TEC target. The construct bound at the cellular membrane is quite stable as it maintains its integrity for several hours. At the imaging field used in this work (7 T), the relaxation efficiency of Gd-loaded apoferritin is only four to five times higher than that of free Gd-HPDO3A. Nevertheless, an ~30% enhancement of SI (after 5 hours) was observed upon administering doses of Gd (0.01 mmol/kg) that are more than 1 order of magnitude lower than the doses currently used for Gd-HPDO3A in clinical protocols.

The *in vivo* biodistribution of Gd-Apo-Bio shows that the modified protein is absorbed by the hepatocytes as the native protein, thus demonstrating that the portion involved in the binding with its receptors is substantially unchanged. Finally, the entrapment of different molecules in the apoferritin cavity (using the method described above) can be exploited to transform the protein in a carrier of both diagnostic and therapeutic agents. This observation promotes the apoferritin-based delivery system as a good alternative to the liposomes or nanoparticles as a dual probe for imaging and therapy, opening the interesting field of MRI-guided targeted drug delivery.

In conclusion, Gd-loaded apoferritin displays enough sensitivity to allow the MRI visualization of human tumor–derived endothelial cells transplanted into mice and targeted with a biotinylated peptide that binds to the selective surface molecule NCAM. In principle, the same procedure can be extended to a number of biotinylated targeting vectors, i.e., peptides and peptido mimetics, oligosaccharides, as well as larger macromolecules such as proteins and antibodies. Gd-loaded apoferritin recalls, to same extent, properties widely exploited with liposomes and other vesicle-like systems but with the advantage of having a smaller size (12-15 nm), thus improving its accessibility to targets outside the bloodstream. As apoferritin can be loaded with other molecules, one may envisage a more extensive use for this carrier system in several molecular imaging protocols. This approach can be exploited for the detection of tumor angiogenesis, for the evaluation of the effect of antiangiogenic therapy, as well as coupling the vector with drugs, for direct imaging, and quantification of drug delivery.

Acknowledgments

Received 5/11/2006; revised 7/5/2006; accepted 7/20/2006.

Grant support: Italian Ministry of University and Research: FIRB project (RBNE01HRS5-001, RBNE01ZL3R-001) and PRIN, Regione Piemonte-Ricerca Scientifica Applicata and by Progetto S. Paolo Oncologia, Associazione Italiana per la Ricerca sul Cancro, and has been carried out under the frame of COST D18 Action, EMIL, and DiMI EU NoEs. Support from Bracco Imaging S.p.A. is gratefully acknowledged.

The costs of publication of this article were defrayed in part by the payment of page charges. This article must therefore be hereby marked *advertisement* in accordance with 18 U.S.C. Section 1734 solely to indicate this fact.

DOI:10.1158/0008-5472.CAN-06-1728

References

1. Rinck PA. Magnetic Resonance in Medicine. Oxford: Blackwell Scientific Publications; 2003.
2. Merbach AE, Toth E. The chemistry of contrast agents in medical magnetic resonance imaging. Chichester (United Kingdom): John Wiley & Sons; 2001.
3. Caravan P, Ellison JJ, McCurry TJ, Lauffer RB. Gadolinium (III) chelates as MRI contrast agents: structure, dynamics and applications. Chem Rev 1999; 99:2293–352.
4. Artemov D, Bhujwalla ZM, Bulte JW. Magnetic resonance imaging of cell surface receptors using targeted contrast agents. Curr Pharm Biotechnol 2004; 5:485–94.
5. Aime S, Cabella C, Colombatto S, Geninatti Crich S, Gianolio E, Maggioni F. Insights into the use of paramagnetic Gd(III) complexes in MR-molecular imaging investigations. J Magn Reson Imaging 2002;16: 394–406.
6. Winter PM, Caruthers SD, Wickline SA, Lanza GM. Molecular imaging by MRI. Curr Cardiol Rep 2006;8:65–9.
7. Weissleder R, Mahmood U. Molecular imaging. Radiology 2001;219:316–33.
8. Aime S, Frullano L, Geninatti Crich S. Compartmentalization of a gadolinium complex in the apoferritin cavity: a route to obtain high relaxivity contrast agents for magnetic resonance imaging. Angew Chem Int Ed Engl 2002;41:1017–9.
9. Padhani AR, Neeman M. Challenges for imaging angiogenesis. Br J Radiol 2001;74:886–90.
10. Neeman M. Preclinical MRI experience in imaging angiogenesis. Cancer Metastasis Rev 2000;19:39–43.
11. Carmeliet P. Angiogenesis in health and disease. Nat Med 2003;9:653–60.
12. Carmeliet P, Jain RK. Angiogenesis in cancer and other diseases. Nature 2000;407:249–57.
13. Brooks PC, Clark RAF, Cheresh DA. Requirement of vascular integrin $\alpha v\beta 3$ for angiogenesis. Science (Washington DC) 1994;264:569–71.
14. Sipkins DA, Cheresh DA, Kazemi MR, Nevin LM, Bednarski MD, Li KC. Detection of tumor angiogenesis *in vivo* by $\alpha v\beta 3$-targeted magnetic resonance imaging. Nat Med 1998;4:623–6.
15. Winter PM, Caruthers SD, Kassner A, et al. Molecular imaging of angiogenesis in nascent Vx-2 rabbit tumors using a novel $\alpha(v)\beta 3$-targeted nanoparticle and 1.5 tesla magnetic resonance imaging. Cancer Res 2003; 63:5838–43.
16. Schmieder AH, Winter PM, Caruthers SD, et al. Molecular MR imaging of melanoma angiogenesis with $\alpha v\beta 3$-targeted paramagnetic nanoparticles. Magn Reson Med 2005;53:621–7.
17. Mulder WJ, Strijkers GJ, Habets JW, et al. MR molecular imaging and fluorescence microscopy for identification of activated tumor endothelium using a bimodal lipidic nanoparticle. FASEB J 2005;19:2008–10.
18. Montet X, Montet-Abou K, Reynolds F, Weissleder R, Josephson L. Nanoparticle imaging of integrins on tumor cells. Neoplasia 2006;8:214–22.
19. Mulder WJ, Strijkers GJ, Griffioen AW, et al. A liposomal system for contrast-enhanced magnetic resonance imaging of molecular targets. Bioconjug Chem 2004;15:799–806.
20. Sibson NR, Blamire AM, Bernades-Silva M, et al. MRI detection of early endothelial activation in brain inflammation. Magn Reson Med 2004;51:248–52.
21. Sipkins DA, Gijbels K, Tropper FD, Bednarski M, Li KC, Steinman L. ICAM-1 expression in autoimmune encephalitis visualized using magnetic resonance imaging. J Neuroimmunol 2000;104:1–9.
22. Bussolati B, Deambrosis L, Russo S, Deregibus MC, Camussi G. Altered angiogenesis and survival in human tumor-derived endothelial cells. FASEB J 2003;17:1159–61.
23. Rønn LCB, Berezin V, Bock E. The neural cell adhesion molecule in synaptic plasticity and ageing. Int J Dev Neurosci 2000;18:193–9.
24. Bussolati B, Grange C, Bruno S, et al. Neural-cell adhesion molecule (NCAM) expression by immature and tumor-derived endothelial cells favors cell organization into capillary-like structures. Exp Cell Res 2006; 312:913–24.
25. Rønn LCB, Olsen M, Ostergaard S, et al. Identification of a neuritogenic ligand of the neural cell adhesion molecule using a combinatorial library of synthetic peptides. Nat Biotechnol 1999;17:1000–5.
26. Rønn LCB, Dissing S, Holm A, Berezin V, Bock E. Increased intracellular calcium is required for neurite outgrowth induced by a synthetic peptide ligand of NCAM. FEBS Lett 2002;518:60–6.
27. Kiryushko D, Kofoed T, Skladchikova G, Holm A, Berezin V, Bock E. A synthetic peptide ligand of NCAM, C3d, promotes neuritogenesis and synaptogenesis and modulates presynaptic function in primary cultures of rat hippocampal neurons. J Biol Chem 2003;278: 12325–34.
28. Berezin V, Bock E. NCAM mimetic peptides. J Mol Neurosc 2003;22:33–9.
29. Hermanson GT. Bioconjugate techniques. San Diego: Academic Press, Inc.; 1996.
30. Bradford MM. A rapid and sensitive method for the quantitation of microgram quantities of protein utilizing the principle of protein-dye binding. Anal Biochem 1976;72:248–54.
31. Vasalatiy O, Zhao P, Zhang S, Aime S, Sherry AD. Catalytic effects of apoferritin interior surface residues on water proton exchange in lanthanide complexes. Contrast Med Mol Imaging 2006;1:15–22.
32. Eakins MN, Eaton SM, Fisco RA, et al. Physicochemical properties, pharmacokinetics, and biodistribution of gadoteridol injection in rats and dogs. Acad Radiol 1995; 2:584–91.
33. Soltys RA. Summary of preclinical safety evaluation of gadoteridol injection. Invest Radiol 1992;27:S7–11.
34. Debatin JF, Nadel SN, Gray L, et al. Phase III clinical evaluation of gadoteridol injection: experience in pediatric neuro-oncologic MR imaging. Pediatr Radiol 1992;22:93–8.
35. Crichton RR. Proteins of iron storage and transport. Adv Protein Chem 1990;40:281–363.